Characterization of Piezoelectric Microgenerator with Nanobranched ZnO Grown on a Polymer Coated Flexible Substrate

Mariya Aleksandrova [1,*] **, Georgi Kolev** [1], **Yordanka Vucheva** [1], **Habib Pathan** [2]
and Krassimir Denishev [1]

[1] Department of Microelectronics, Technical University of Sofia, 1000 Sofia, Bulgaria;
    georgi_klv@abv.bg (G.K.); y.vucheva@gmail.com (Y.V.); khd@tu-sofia.bg (K.D.)
[2] Department of Physics, Savitribai Phule Pune University, Pune 411007, India; pathan@physics.unipune.ac.in
[*] Correspondence: m_aleksandrova@tu-sofia.bg; Tel.: +359-2965-3085

Featured Application: The application of the proposed device is for the energy-harvesting element of a flexible piezoelectric microgenerator. It could serve as a self-sufficient power supply for portable devices working in the frequency range of 10 Hz to 10 kHz, such as biomedical microsensors, tracking devices, and other wearable electronics that are mechanically activated by human motions.

Abstract: In this paper, results from the fabrication and study of a piezoelectric microgenerator using nanobranched zinc oxide (ZnO) film grown on poly(3,4-ethylenedioxythiphene) doped with a sulfonate (PEDOT:PSS)-coated flexible substrate are presented. The aim of the study is to extract information about the electrical behavior of the harvester at different frequencies, temperatures, and positions, as related to the ZnO nanostructure, as well as to examine its piezoelectric response. Radiofrequency (RF) sputtering with oxygen deficit during growth on an amorphous sublayer was used to obtain the nanobranched structure. The microdevice was studied at frequencies ranging from 1 Hz to 1 MHz for temperatures in the range of $-10\,^\circ$C to $40\,^\circ$C, in both a non-bended position, and a radius of curvature position bended to 12 mm. It was found that non-ordered ZnO nanoformations facilitate the dipoles' motion, thus leading to low dielectric losses of 10^{-3}, and a higher relative permittivity of ε_r ~15, compared with typically known values. The losses increase with one order of magnitude at bending, but still remain low. Dielectric characteristics indicate that the favorable working range of the microgenerator is within the lower frequency region, from 10 Hz to 10 kHz. The results were confirmed by the measured open circuit voltage, which reaches approximately 1 V within this range, versus 300 mV out of the range.

1. Introduction

Recently, there has been a growing interest in energy-harvesting devices, and particularly piezoelectric ones that scavenge the vibrations, force, or pressure changes from the ambient. The advanced nanomaterials and technologies allow such devices to be very thin, lightweight, compact, and even flexible [1–3]. The potential applications of such microdevices could be for the self-sufficient power supply of biomedical microsensors attached to the human body and reacting to blood pressure changes [4], in the security sector as a part of the tracking devices [5], in everyday life by incorporating

them in clothes and shoes (wearable piezoelectric harvesters) for activation from the body movements, implanted underneath the keyboard of a PC/laptop [6], etc.

A key moment in the development and optimization of the thin film piezoelectric energy harvestings was the enhancement of their relatively low conversion efficiency. This problem has deepened in the last few years due to replacing the most efficient piezoelectric coating of lead-zirconium titanate (PZT) [7] with lead-free materials, which are less effective. Vibration-activated microgenerators can provide a power output of ~4 µW for the range of low frequencies that correspond to human motion, and up to 800 µW if they are stimulated by the high frequencies of machine motions [8]. Zinc oxide (ZnO) is among the environmentally friendly and cost-effective materials that exhibit piezoelectric properties. It is characterized with a piezoelectric coefficient of about 12 pC/N, a bandgap of 3.37 eV at room temperature, and relative dielectric permittivity of ε_r = 8.75 [9]. Different growing techniques have been used to deposit thin nanostructured ZnO films, because it was found that the piezoelectric coefficient is much higher for nanostructures than bulk wurtzite structures. However, most of the films' deposition methods are not compatible with the conventional microdevices fabrication technology or cannot be applied to the flexible substrates due to elevated temperatures or unwanted chemical reactions. Such methods include, for example, hydrothermal [10], the reduction of ZnO powder by H_2 [11], and the seedless chemical approach [12]. From the other side, there are available data for the application of chemical vapor deposition (CVD) [13] and Radiofrequency (RF) sputtering [14]. A variety of harvesting designs with incorporated ZnO films have been proposed in the literature; however, different problems have arisen, such as low electromechanical coupling, low dielectric permittivity, high dielectric losses, and high mechanical instability at bending, twisting and/or stretching. These problems prevent the commercial implementation of ZnO, and further optimization is required. One of the successful approaches to improve ZnO piezoelectric behavior is to form nanostructures such as nanowires, nanorods, nanoflowers, nanobelts, and other three-dimensional (3D) film structures that can be tuned by the growing mode in order to facilitate the polarization of the media [15–17]. Some of these microsystems have narrow frequency ranges (from few tenth of Hz to few KHz) that are usually limited to the resonance frequency [18]. Lee et al. [19] demonstrated a fully stand-alone, self-powered sensor device, powered by a ZnO nanowire array on a flexible Kapton substrate. The mechanical bending of this microgenerator resulted in an output voltage of about 350 mV and a current density of 125 nA/cm^2. Zhao et al. [20] achieved a high effective piezoelectric coefficient for ZnO nanobelts that varied with the frequency between 14.3 pm/V and 26.7 pm/V, which confirmed the possible application of these nanostructures as nanosensors and nanoactuators. Some articles are devoted to the investigation of the size effect on the piezoelectric response for ZnO nanowires and nanobelts, which is also important for energy-harvesting devices [21,22].

Another important issue is the mechanical stability of microdevices subjected to continuous vibrations, especially when they are deposited on flexible substrates. Oxide materials are brittle, and bending over more than 1000–2000 cycles can causes microcracks in the films, complete physical degradation, and failure of the device. In order to reduce the difference in the Young modulus of the flexible substrate and the oxide piezoelectric films, supplementary polymer nanoparticles are added as intermediate nanocoatings formed hybrid organic/inorganic interfaces. Another approach is to use blends for making nanocomposite ZnO/polymer [23,24]. Their function in the device is to pick up plastic deformations and decrease stress. In addition, the substrate/sublayer materials and their structures play an important role in the determination of the ZnO nanostructures [25]. It is preferable to use conductive polymers such as poly(3,4-ethylenedioxythiphene) doped with polystyrene sulfonate (PEDOT:PSS) and polypyrrole (PPY) to avoid electrical isolation of the electrodes, or to serve as electrodes by themselves. It was demonstrated that PEDOT:PSS is the most frequently used polymer in combination with the most spread flexible substrate of polyethylene terephthalate (PET), due to the favorable wetting conditions of the PET surface from the PEDOT:PSS solution, and good adhesive strength of the polymer coating to PET [26].

In this study, ZnO film was sputtered on a PEDOT:PSS-coated PET substrate at modified deposition mode with oxygen deficit in order to obtain a 3D nanobranched structure. The structure is intended to serve as a piezoelectric microgenerator. The function of PEDOT:PSS is to enhance the mechanical stability of the entire microdevice, and to serve as an amorphous sublayer for non-ordered ZnO growth. It is believed that in this way, the obtained laterally aligned nanobranches on a bendable substrate will be subjected to maximal deformation without incurring a fast degradation process. The aim of using nanobranched ZnO is to facilitate the dipoles' orientation and their movement to the electrical poles, which is expected to decrease dielectric losses. In order to extract information about the dielectric behavior of the microdevice, dielectric losses are measured at different frequencies from 1 Hz to 1 MHz, and for temperatures ranging from $-10\ ^\circ$C to 40 $^\circ$C. Relative permittivity ε_r is calculated for the same values. Structures' workability is demonstrated by presenting the generated voltage oscillograms. The processes and the curve trends are discussed with regard to the ZnO microstructure and its morphology. The significance of the work consists of the finding of new knowledge about the novel nanobranched piezoelectric structures with polymeric electrodes, and defining their frequency and temperature working range, thus determining their potential application.

2. Materials and Methods

Flexible polyethylene terephthalate (PET) is used as a substrate material for the piezoelectric harvesting devices. Poly(3,4-ethylenedioxythiophene) polystyrene sulfonate (PEDOT:PSS) solution with 1.3% conductivity grade was spin-coated on PET at 2500 rpm per 30 s, and dried at 90 $^\circ$C to remove the residual solvent. The resulting film has a thickness of 40 nm and exhibits a sheet resistance of 85 Ω/sq. A ZnO film with a thickness of 550 nm was deposited directly on the polymer-coated PET without a seed layer by RF sputtering with additional oxidation of the target. The specific sputtering power was 405 mW/cm^2, the sputtering argon gas pressure was 2.10^{-2} Torr, and the oxygen pressure initially was higher (8×10^{-4} Torr), with a continuous decrease down to 2×10^{-4} Torr by the end of the sputtering. Thus, the initial monolayers with high density served as seed for assistance of the ZnO growth. Further, the oxygen deficit resulted in vacations in the lattice and hollow formations between the nanobranches. PEDOT:PSS was spin-coated on the ZnO film at the same deposition conditions as for the bottom electrode, in order to make the contacting surface between ZnO and the top electrode smoother and flatter. As well, in this way, the diffusion of nanoparticles between the nanobranches, originating from the top electrode and moving toward the bottom electrode, is prevented. A top Au electrode with a thickness of 90 nm was deposited by low-temperature DC sputtering. Figure 1a presents the layered structure of the flexible nanobranched harvester.

The ZnO surface morphology was analyzed by scanning electron microscopy (SEM, JSM-6390LV, JEOL, Peabody, MA, USA). X-ray diffraction (XRD, D8 ADVANCE, Bruker, Karlsruhe, Germany) was used to determine the presence of piezoelectric features. Dielectric characterization of the fabricated prototype was made by resistance-inductance-capacitance RLC type measurements (Instek LCR 819, Good Will Instrument Co., Ltd., New Taipei City, Taiwan) for estimation of the structures' capacitance (relative permittivity is provided as plots, based on calculations, using the capacitance values), and dielectric losses in the frequency range 1 Hz–1 MHz for extracting information about the quality of the piezoelectric film and the polarization processes in the microdevice. Additionally, the same measurements were completed at different temperatures in the range of -10 to 40 $^\circ$C, which are the typical ambient temperatures for the intended potential application of the proposed harvester. The measurements were conducted for the two basic states of the samples: non-bended (flat), and continuously bended at a radius of 12 mm (curved), in order to provide data about the change in the dielectric behavior after mechanical loading. The piezoelectric response of the structure was recorded by digital oscilloscope (DQ2042CN Shanghai MCP Corp., Shanghai, China) at an applied cyclic mechanical stimulus (tension/compression stress of the sample) of 350 g forces with tunable frequency. The electromechanical system for the stimulation of charges by bending is lab-made, where a motor is activated by a power source and a signal generator regulates the frequency of the

vibrating cantilever. The samples were attached on the top of this cantilever. A photo of the setup for mechanical test is presented in Figure 1b,c which shows the stress zones over the samples at static bending. All measurements were conducted without preliminary poling of the samples.


(**a**)

(**b**)

(**c**)
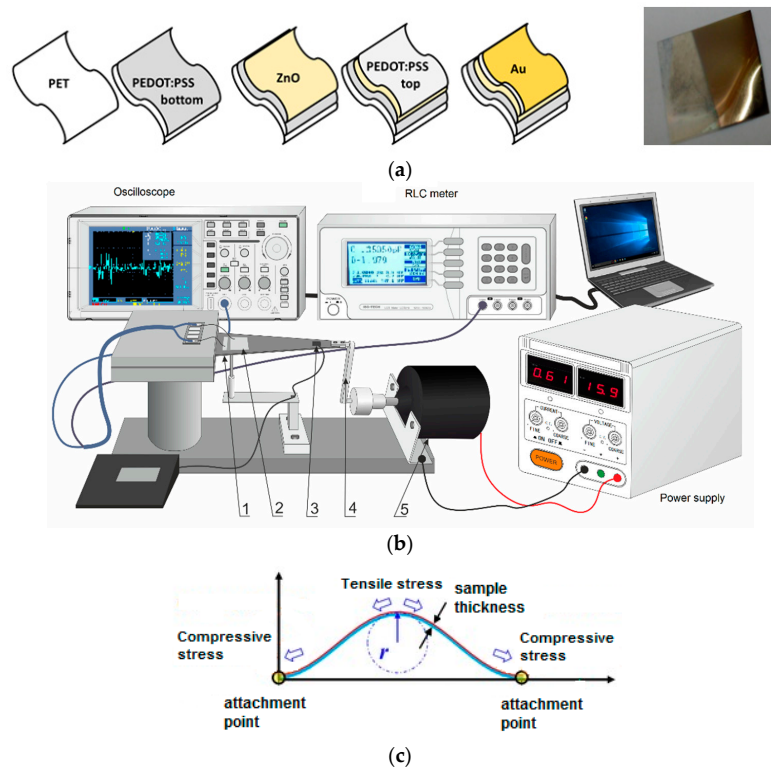
Figure 1. Schematics of (**a**) a layered configuration of the flexible polymer-based piezoelectric harvester (**left**) and photo of the sample (**right**); (**b**) lab-made combined vibrational setup and cyclic bend tester (1—beam, 2—sample under test, 3—weight detector, 4—tiller bending the beam, 5—electromotor activating the tiller); (**c**) sample configuration at static bent conditions with a certain radius of curvature.

3. Results and Discussion

Figure 2 shows the X-ray diffraction (XRD) spectrum of the zinc oxide nanobranched structure, which was similar to that of the wurtzite structure. Although some of the peaks, such as (200) and (103) corresponding to the ZnO crystalline structure are missing from the pattern, the peaks of some main phases responsible for the piezoelectric response, such as (100), (102) and (110) presented, and indicated a non-centrosymmetric structure for ZnO [27]. A modified pattern could be ascribed to the amorphous polymer-contained electrode, which could serve as a base for the ZnO film sputtering without an auxiliary seed sublayer. This is also the reason for randomly oriented ZnO nanobranches grown on the amorphous substrate [25]. For the nanobranched ZnO, there is a slight shift of the highest intensity peak from 30° toward lower angles 2θ of 27° when compared with other ZnO nanostructures (nanowires, nanorods, etc.). This is evidence for an increase in the nanoformations spacing (distance between planes), which induces uniform tensile strain in the nanobranches due to the dislocated growth of the side dendrites [28]. The strain is calculated to be 0.94×10^{-3}, following the formula $\varepsilon = \frac{\beta}{4tan\theta}$, where β is the measured broadening of the major diffraction line peak at an angle of 2θ, at half its maximum intensity, and θ is the Bragg diffraction angle of the XRD peak. Nevertheless, this value is much lower than some cases reported in the literature, which were obtained as a result of lattice unit cell expansion due to high deposition temperature or doping process; as a result, it can be assumed that the electromechanical performance of the film will not be affected [29]. Moreover, it is

suggested that such low density film could be easy polarizable, and the dipoles formation and voltage generation processes will be strongly alleviated, which will cause dielectric losses to decrease.
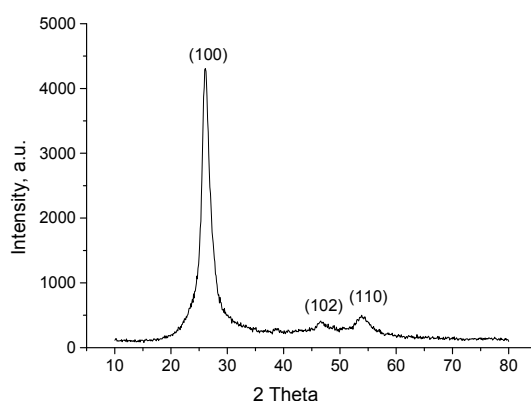
Figure 2. X-ray diffraction (XRD) pattern of nanobranched zinc oxide (ZnO) grown on poly(3,4-ethylenedioxythiphene) doped with a polystyrene sulfonate (PEDOT:PSS)-coated flexible substrate of polyethylene terephthalate (PET).

The surface morphology of the ZnO nanobranched film was characterized by using scanning electron microscopy (SEM), and the image is shown in Figure 3. The film consists of long wires with a length of few micrometers, a diameter of ~150–200 nm, and side grown dendrites, all forming configuration that resemble leaf. Each of the side growths has a different length, varying from 500 nm to 1.5 μm, but their thickness seems to be one and the same: approximately 100 nm. All nanoformations are merged into a loose network. The exact mechanism of the side dendrites formation should be further examined. The branched structure has no preferable growth direction and no alignment; they are randomly oriented. This is in good agreement with the XRD pattern, and indicates relatively poor crystallinity. The reason could be the non-crystalline substrate/polymer electrode, which is the base for further revealing of the nanostructure. In our previous study [30], we showed that a very similar ZnO texture can be used to enhance the piezoelectric response of unit piezoelectric film thickness, due to the contribution of the dendrites to the process of electrical poles formation. Further, the structural and morphological results are correlated with dielectric studies. It was also proved that such an element generates piezoelectric voltage at more than one frequency of the mechanical stimulus and can work in a non-resonance mode.
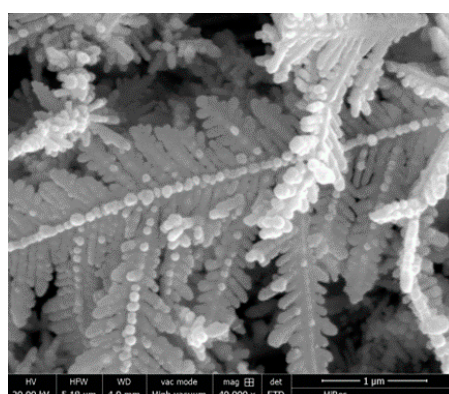
Figure 3. Scanning electron microscopy (SEM) image of the surface morphology of nanobranched ZnO grown on a PEDOT:PSS-coated flexible substrate of PET.

In order to take advantage of a nanobranched structure for potential applications in energy-harvesting devices, its electrical behavior has to be studied in detail to clarify the interactions

between the dipole formations and the nanobranches. For this purpose, the permittivity (ε_r) and the dielectric losses (tan δ) were measured at different frequencies (f) and temperatures (T), as well as at static mechanical load (continuous bended position). The device with nanobranched ZnO showed significantly enhanced relative permittivity compared with dense ZnO and ZnO composites prepared for improving the piezoelectric response [31]. Figure 4a shows that all curves exhibit a similar trend of gradual decrease along with the frequency, with a more significant difference in the values at the negative temperature of −10 °C. Figure 4b shows that in the frequency range of 20 Hz–20 kHz, little difference can be observed in the curves measured at different temperatures. This may be because all of the nanobranches are similar lengths. This can be confirmed from the SEM image shown previously, where not much difference can be observed between the separate nanoformations.
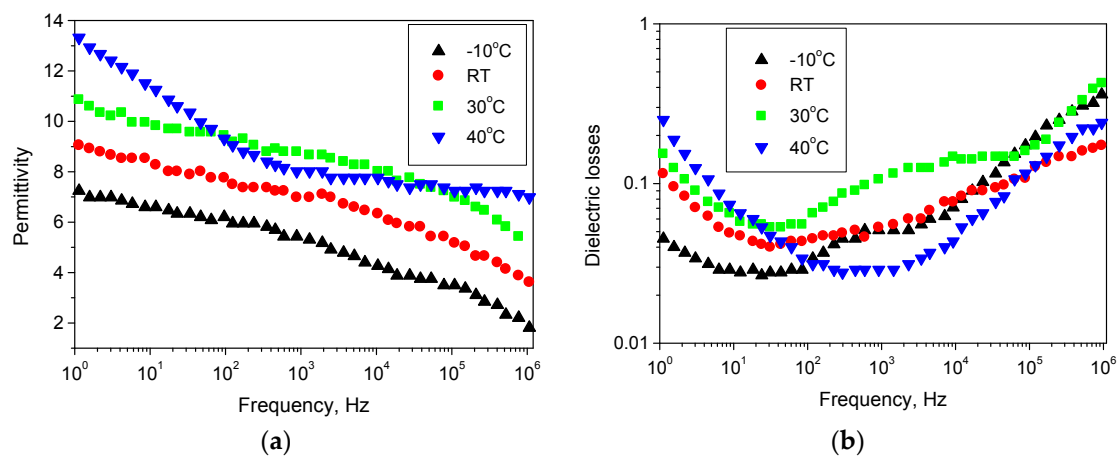

(a)

(b)
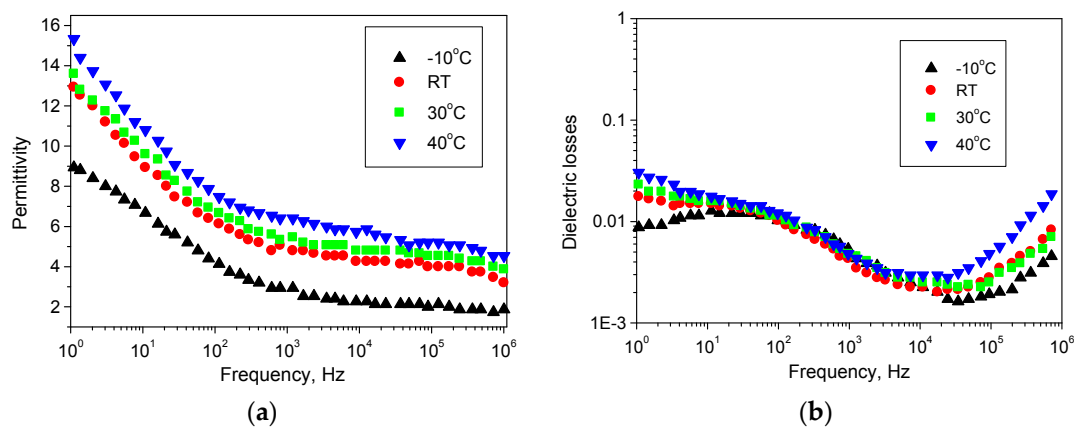
Figure 4. Frequency dependence of the (**a**) relative permittivity and (**b**) dielectric losses at different temperatures for the non-bended sample PET/PEDOT:PSS/ZnO/PEDOT:PSS/Au.

Dielectric losses indicate that a decrement with almost one order of magnitude can be seen in the lower frequency region from a few Hz up to 10 kHz, except for the negative temperature (−10 °C), where first there is a small increment in the lowest frequency range. All curves follow a similar trend for frequencies higher than 10 kHz. The dielectric losses increase with the temperature (and with the frequency). The higher values at the lower frequency region are related to the electric energy converted into heat loss when the electric field is applied, probably due to impossibility of the dipoles to move fluently among the branched media when no stress (displacement) is applied. The higher values of the dielectric losses at frequencies higher than 30 kHz occurred because of the low dipoles mobility, which prevented any following of the fast changes of the stimulus polarity. The relative permittivity decreased sharply up to 200 Hz, and after that slowed down. This is due to the dipoles' low mobility; because they do not have much time to polarize the media at higher frequencies, weak dependence of the permittivity on the frequencies was observed. The higher permittivity of the nanobranched ZnO (ε_r ~15) compared with the typical values known (ε_r ~9) is probably due to high branch interfacial polarization, which causes an accumulation of charges at the interfaces between each side dendrite and the main core. The dielectric permittivity increased with the temperature increase, too. This can be ascribed to improving the crystallinity, which leads to stronger interfacial polarization.

The results from the relative permittivity and dielectric losses measurements of the bended piezoelectric microgenerator samples are shown in Figure 5a,b. They indicate that the bended sample shows a lower permittivity than the case before mechanical loading. This can be ascribed to the dipoles' displacement, and the decrease of the distance between them after deformation [32]. This effect is enhanced by the non-centrosymmetric microstructure of the ZnO due to additional polarization induced by the strain gradient across the sample length (the mechanical loading is different at the maximum curvature and at the attachment points of the samples to the measurement setup). Nevertheless, the relative change of the permittivity is not greater than 13%, and is without deviation

of the temperature dependence of the permittivity. The stability in the ε_r-f-T characteristics is due to the mechanical stability of the structure from using PEDOT:PSS as electrodes. It was proven that the excellent elastic properties of the substrate/polymeric electrode system, and specifically PET/PEDOT:PSS, are responsible for stable contact resistance and dynamic capacitance in the flexible electronic devices, thus leading to stable electrical characteristics at bending [33]. Tan δ for the bended samples increased an average of one order of magnitude for the different frequencies and temperatures, showing that the electrical processes revealed in the nanobranched structure are also accomplished by a higher heat loss. In addition, there is a shift in their minimum values to the lower frequencies. After removing the bending force, it was noted that the characteristics restore their initial shape without hysteresis. In general, the dielectric losses for the harvesting device with nanobranched ZnO are smaller than those reported in the literature for devices with high surface-to-volume ratios of the piezoelectric film nanostructure, such as nanowire clusters, for example [34]. This is due to the presence of non-tightly packaged nanoformations, which allow for fluent dipoles orientation and low resistance during polarization. As a result, the generated voltage reached a value more than three times higher than the typical high-density ZnO piezoelectric film's structure, as shown in Figure 6.

Figure 5. Frequency dependence of the (**a**) relative permittivity and (**b**) dielectric losses at different temperatures for bended sample PET/PEDOT:PSS/ZnO/PEDOT:PSS/Au.
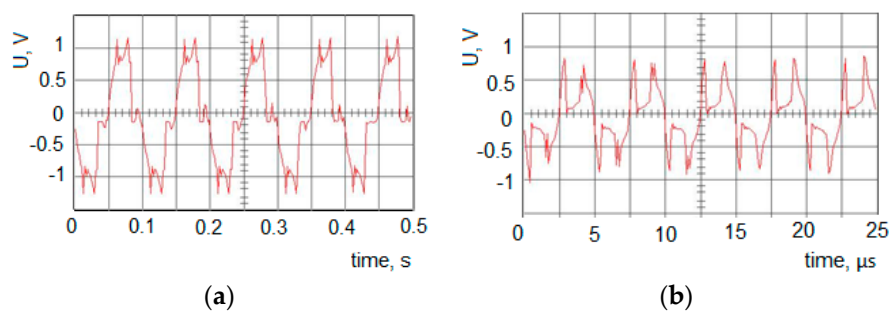

Figure 6. Oscillograms of the generated piezoelectric voltage at frequencies, corresponding to the low (**a**) and high (**b**) dielectric losses regions.

In order to demonstrate the ability of the samples to be used as energy-harvesting devices at low frequencies of mechanical stimulus, the oscillograms of the generated piezoelectric voltage were presented at two frequencies: -10 Hz and 200 kHz. They were selected from the frequency range where the dielectric losses are minimal (0.04–0.05 (Figure 6a) and 0.2), or close to maximal (Figure 6b) at cyclic bending conditions and room temperature. The set mechanical loading in this case is 350 g force units, and the deflection radius is 12 mm. The Y-scale is 500 mV/div for each oscillogram.

Thus, in the low frequency region, the open circuit voltage can reach approximately 1 V. In the higher frequencies region, due to the increased dielectric losses and worsening electromechanical coupling, it can reach an average of 300 mV. The harmonic distortions of the signal are due to the rough nature of the ZnO film surface. Although the top casted PEDOT:PSS solution is highly viscous in order to make the ZnO surface smoother and flatter, it seems that still, the ZnO contacts irregularly with the top electrode coatings.

For estimation of the flexible microgenerator's stability, two types of tests were performed: a dynamic test at a frequency of bending 10 Hz and a mechanical load of 350 g force units, at which the generated signal is the strongest, and a static test (without cyclic repeating bends). In the first case (Figure 7a), soon after the 10,000th bend (equivalent to ~17 h duration of intensive cyclic bending without interruption), the structure sharply exhibited zero current flow similarly to open circuit behavior. This is probably due to electrode failure caused by microcracks occurring in the electrode films, which deteriorate the charge carriers' path to the electrical poles. Such an effect has been reported earlier for flexible devices using PEDOT:PSS-based electrodes on a PET substrate studied at similar test conditions [35]. To confirm this assumption, Figure 7a shows the relative change of the bottom electrode's sheet resistance at different numbers of bends, together with the curve of the current flowing through the whole device. After 1500 bends, the electrode's resistance change against its initial value is less than 25%. Afterward, the sheet resistance remains relatively stable up to 10,000 cycles, with a variation of 7%. The moment of the current dropping down coincides with the sudden resistance change to almost 80%. At this point, the measured sheet resistance of the bottom electrode is almost 4 kΩ, which is an indication of the physical degradation of this film. Although scanning electron microscopic images of the ZnO nanobranched surface after bending are required for clarification of the process, we believe that the ZnO film remains still undamaged. In the second case (Figure 7b), the structure was constantly loaded with increasing mass weight and the voltage change was detected. As can be seen, the generated piezoelectric voltage increased exponentially with the mass load for the ZnO nanobranched-based harvesting. After around 3 kg of loading, the voltage reached approximately 1.4 V; afterward, at 3.6 kg, it dropped abruptly to zero. Separate microscopy testing of the bottom electrode film (not shown) demonstrated that degradation is not observed at this weight. Therefore, the sharp voltage drop to zero can be ascribed to ZnO nanobranched film rupture, and 3.6 kg can be considered a critical working mass load.

(a)   (b)
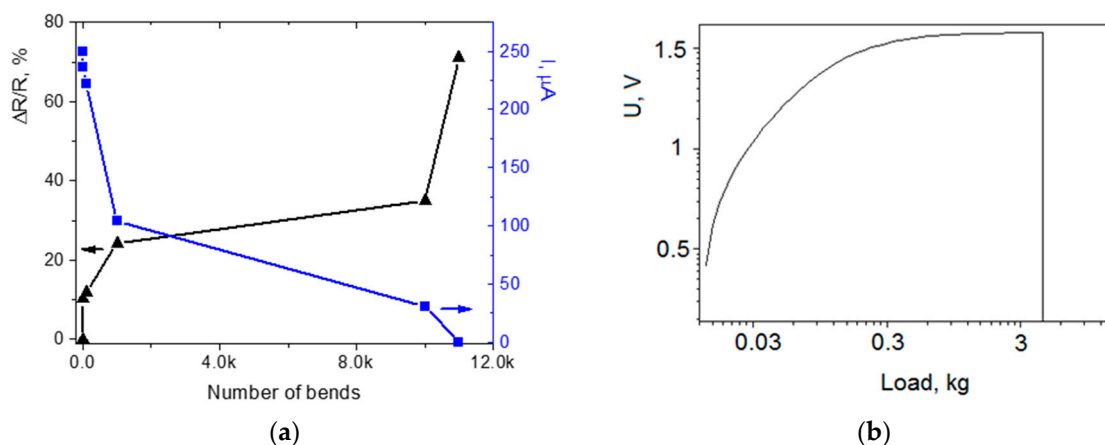
Figure 7. (**a**) Change of the current flow through the multilayer structure and the electrode sheet resistance as a function of the number of bends at a constant frequency of 10 Hz, and (**b**) relation between the voltage generated and the weight at static load.

4. Conclusions

In this study, nanobranched ZnO is obtained by conventional microfabrication technology of ZnO target sputtering on a polymer-coated flexible substrate in oxygen ambient pressure. This is the preferred approach for the mass production of inorganic films for current polymer-based flexible devices containing hybrid interfaces (organic/inorganic). Results indicated that changes in electrical characteristics occur at bending applied without irreversible deterioration. Although the samples exhibit workability in a broad frequency and temperature range (1 Hz to 1 MHz; $-10\,°C$ to 40 $°C$), they are most suitable for flexible piezoelectric energy-harvesting devices in the low and middle frequency region of bending (10 Hz–10 kHz) and temperatures around 20–30 $°C$, where their electrical characteristics are optimal. The critical limits for the device functioning in terms of mechanical loading are 11,000 bends at dynamic loading (350 gr mass loading and 10 Hz cyclic repeating of the loading), and 3.6 kg at static loading. Future work will be related to the investigation of the piezoelectric response as a function of a poling voltage and the detailed study of the degradation processes in the separated layers.

Author Contributions: Mariya Aleksandrova and Krassimir Denishev designed the experiments; Mariya Aleksandrova conducted the generator layer-by-layer fabrication, conducted measurements of dielectric losses at all temperatures for static bended condition and wrote a major part of the paper; Georgi Kolev conducted the measurements of the generated piezoelectric voltage and capacitance (for the permittivity calculations) at different frequencies and analyzed the data; Yordanka Vucheva measured the dielectric losses at non-bended position of the sample, calculated dielectric permittivity for all cases and analyzed the data; Habib Pathan conducted spectroscopic and microscopic measurements of the films and analyzed the data; Krassimir Denishev analyzed the data and wrote some parts of the paper.

Conflicts of Interest: The authors declare no conflict of interest.

References

1. Lee, M.; Chen, C.-Y.; Wang, S.; Cha, S.N.; Park, Y.J.; Kim, J.M.; Chou, L.-J.; Wang, Z.L. A hybrid piezoelectric structure for wearable nanogenerators. *Adv. Mater.* **2012**, *24*, 1759–1764. [CrossRef] [PubMed]

2. Briscoe, J.; Dunn, S. Piezoelectric nanogenerators—A review of nanostructured piezoelectric energy harvesters. *Nano Energy* **2015**, *14*, 15–29. [CrossRef]

3. Park, K.-I.; Jeong, C.K.; Kim, N.K.; Lee, K.J. Stretchable piezoelectric nanocomposite generator. *Nano Converg.* **2016**, *3*, 1–12. [CrossRef] [PubMed]

4. Nanda, A.; Karami, M.A. Energy harvesting from arterial blood pressure for powering embedded micro sensors in human brain. *J. Appl. Phys.* **2017**, *121*, 124506. [CrossRef]

5. Srinandhini, K.; Gnanaprabha, G.; Priyadarshini, K.; Sarumathi, C.; Shanmugapriya, B. Tracking system using GPS and GSM energized by piezoelectric crystal embedded in shoe sole. *Int. J. Adv. Res. Electr. Electron. Instrum. Eng.* **2016**, *5*, 2049–2054. [CrossRef]

6. Wacharasindhu, T.; Kwon, J.W. A micromachined energy harvester from a keyboard using combined electromagnetic and piezoelectric conversion. *J. Micromech. Microeng.* **2008**, *18*, 104016. [CrossRef]

7. Park, K.I.; Son, J.H.; Hwang, G.-T.; Jeong, C.K.; Ryu, J.; Koo, M.; Choi, I.; Lee, S.H.; Byun, M.; Wang, Z.L.; et al. Highly-efficient, flexible piezoelectric PZT thin film nanogenerator on plastic substrates. *Adv. Mater.* **2014**, *26*, 2514–2520. [CrossRef] [PubMed]

8. Mitcheson, P.D.; Green, T.C.; Yeatman, E.M.; Holmes, A.S. Architectures for vibration-driven micropower generators. *J. Microelectromech. Syst.* **2004**, *13*, 429–440. [CrossRef]

9. Gao, P.X.; Wang, Z.L. Nanoarchitectures of semiconducting and piezoelectric zinc oxide. *J. Appl. Phys.* **2005**, *97*, 044304. [CrossRef]

10. Opoku, C.; Dahiya, A.S.; Oshman, C.; Cayrel, F.; Poulin-Vittrant, G.; Alquier, D.; Camara, N. Fabrication of ZnO nanowire based piezoelectric generators and related structures. *Phys. Procedia* **2015**, *70*, 858–862. [CrossRef]

11. Burshtein, G.; Lumelsky, V.; Lifshitz, Y. ZnO nanowires growth via reduction of ZnO powder by H_2. *Nanotechnology* **2015**, *26*, 125602. [CrossRef] [PubMed]

12. Xu, S.; Lao, C.; Weintraub, B.; Wang, Z.L. Density-controlled growth of aligned ZnO nanowire arrays by seedless chemical approach on smooth surfaces. *J. Mater. Res.* **2008**, *23*, 2072–2077. [CrossRef]

13. Liu, J.; Wu, W.; Bai, S.; Qin, Y. Synthesis of high crystallinity ZnO nanowire array on polymer substrate and flexible fiber-based sensor. *ACS Appl. Mater. Interfaces* **2011**, *3*, 4197–4200. [CrossRef] [PubMed]

14. Chen, T.-P.; Young, S.-J.; Chang, S.-J.; Hsiao, C.-H.; Hsu, Y.-J. Bending effects of ZnO nanorod metal-semiconductor-metal photodetectors on flexible polyimide substrate. *Nanoscale Res. Lett.* **2012**, *7*, 214–219. [CrossRef] [PubMed]

15. Wu, W.; Huang, X.; Li, S.; Jiang, P.; Toshikatsu, T. Novel three-dimensional zinc oxide superstructures for high dielectric constant polymer composites capable of withstanding high electric field. *J. Phys. Chem. C* **2012**, *116*, 24887–24895. [CrossRef]

16. Al-Ruqeishi, M.S.; Mohiuddin, T.; Al-Habsi, B.; Al-Ruqeishi, F.; Al-Fahdi, A.; Al-Khusaibi, A. Piezoelectric nanogenerator based on ZnO nanorods. *Arab. J. Chem.* **2017**, in press. [CrossRef]

17. Ou, C.; Sanchez-Jimenez, P.E.; Datta, A.; Boughey, F.L.; Whiter, R.A.; Sahonta, S.-L.; Kar-Narayan, S. Template-assisted hydrothermal growth of aligned zinc oxide nanowires for piezoelectric energy harvesting applications. *ACS Appl. Mater. Interfaces* **2016**, *8*, 13678–13683. [CrossRef] [PubMed]

18. Yu, H.; Zhou, J.; Deng, L.; Wen, Z. A vibration-based MEMS piezoelectric energy harvester and power conditioning circuit. *Sensors (Basel)* **2014**, *14*, 3323–3341. [CrossRef] [PubMed]

19. Kim, K.-H.; Lee, K.Y.; Seo, J.-S.; Kumar, B.; Kim, S.-W. Paper-based piezoelectric nanogenerators with high thermal stability. *Small* **2011**, *7*, 2577–2580. [CrossRef] [PubMed]

20. Zhao, M.-H.; Wang, Z.-L.; Mao, S.X. Piezoelectric characterization of individual zinc oxide nanobelt probed by piezoresponse force microscope. *Nano Lett.* **2004**, *4*, 587–590. [CrossRef]

21. Agrawal, R.; Espinosa, H.D. Giant piezoelectric size effects in zinc oxide and gallium nitride nanowires—A first principles investigation. *Nano Lett.* **2011**, *11*, 786–790. [CrossRef] [PubMed]

22. Momenia, K.; Odegard, G.M.; Yassar, R.S. Finite size effect on the piezoelectric properties of ZnO nanobelts: A molecular dynamics approach. *Acta Mater.* **2012**, *60*, 5117–5124. [CrossRef]

23. Kurbanov, M.A.; Bayramov, A.A.; Safarov, N.A.; Tatardar, F.N.; Sultanaxmedova, I.S. Hybrid piezoelectric composites with high electromechanical characteristics. *Sci. Isr. Technol. Advant.* **2012**, *14*, 1–6.

24. Thakur, V.K.; Thakur, M.K.; Gupta, R.K. *Hybrid Polymer Composite Materials: Processing*; Woodhead Publishing: Cambridge, UK, 2017; ISBN 9780081007877.

25. Comedi, D.; Tirado, M.; Zapata, C.; Heluani, S.P.; Villafuerte, M.; Mohseni, P.K.; LaPierre, R.R. Randomly oriented ZnO nanowires grown on amorphous SiO$_2$ by metal-catalyzed vapour deposition. *J. Alloys Compd.* **2010**, *495*, 439–442. [CrossRef]

26. Aleksandrova, M.; Kurtev, N.; Videkov, V.; Tzanova, S.; Schintke, S. Material alternative to ITO for transparent conductive electrode in flexible display and photovoltaic devices. *Microelectron. Eng.* **2015**, *145*, 112–116. [CrossRef]

27. Rao, R.; Sahoo, P.K.; Sukla, R.; Panda, H.S. New approach to anchor zinc oxide in polyvinylidene fluoride and their dielectric properties. *Adv. Sci. Eng. Med.* **2014**, *6*, 166–172. [CrossRef]

28. Chen, H.-W.; Yang, H.-W.; He, H.-M.; Lee, Y.-M. ZnO nanorod arrays prepared by chemical bath deposition combined with rapid thermal annealing: Structural, photoluminescence and field emission characteristics. *J. Phys. D Appl. Phys.* **2016**, *49*, 025306. [CrossRef]

29. Shanmugan, S.; Mohamed Mustaqim, A.B.; Mutharasu, D. Structural parameters analysis of Mg doped ZnO nano particles for various Mg concentrations. *Int. J. Eng. Trends Technol.* **2015**, *28*, 27–36. [CrossRef]

30. Kolev, G.; Aleksandrova, M.; Dobrikov, G.; Pathan, H.; Fartunkov, M.; Denishev, K. Piezoelectric energy harvesting device with nanobranched ZnO on polymer/metal/polymer coated flexible substrate. In Proceedings of the XV-th International Conference on Electrical Machines, Drives and Power Systems ELMA2017, Sofia, Bulgaria, 1–3 June 2017; pp. 320–324.

31. Devi, P.I.; Ramachandran, K. Dielectric studies on hybridised PVDF-ZnO nanocomposites. *J. Exp. Nanosci.* **2011**, *6*, 281–293. [CrossRef]

32. Deng, Q.; Kammoun, M.; Erturk, A.; Sharma, P. Nanoscale flexoelectric energy harvesting. *Int. J. Solids Struct.* **2014**, *51*, 3218–3225. [CrossRef]

33. Aleksandrova, M.; Dobrikov, G.; Singh, A.K.; Videkov, V.; Kolev, G. Flexible optoelectronic device with polymer based electrode on hybrimer substrate. In Proceedings of the 40th International Spring Seminar on Electronics Technology—ISSE2017, Sofia, Bulgaria, 10–14 May 2017.

34. Aepuru, R.; Bhaskara, B.V.; Kale, S.N.; Panda, H.S. Unique negative permittivity of the pseudo conducting radial zinc oxide-poly(vinylidene fluoride) nanocomposite film: Enhanced dielectric and electromagnetic interference shielding properties. *Mater. Chem. Phys.* **2015**, *167*, 61–69. [CrossRef]

35. Aleksandrova, M.; Videkov, V.; Dobrikov, G.; Andreev, S.; Kolev, G.; Ivanova, R. PEDOT:PSS transparent conductive films on flexible substrates for optoelectronic devices application: Impact of the temperature on their electromechanical behavior. *Nanosci. Nanotechnol. Nanostruct. Mater. Appl. Innov. Transf.* **2015**, *15*, 24–27.